Numerical Analysis on the Aerodynamic Characteristics of SUV Car Model Install with Vortex Generator

Muhammad Amirul Hakimin Zainondin[1], Izuan Amin Ishak[1,*], Mohd Fuad Yasak[1], Mohammad Arafat[1], Nor Atiqah Zolpakar[2], Nurshafinaz Mohd Maruai[3]

[1] Faculty of Engineering Technology, University of Tun Hussein Onn Malaysia, Education Hub Pagoh, 84600, Malaysia
[2] Faculty of Mechanical & Automotive Engineering Technology Universiti Malaysia Pahang, 26600 Pekan, Pahang, Malaysia
[3] Department of Mechanical Precision Engineering, Malaysia-Japan International Institute of Technology (MJIIT), Universiti Teknologi Malaysia (UTM), Jalan Sultan Yahya Petra, 54100, Kuala Lumpur, Malaysia

ARTICLE INFO	ABSTRACT
	The investigation of automotive aerodynamics involves analysing several forces operating on a car while driving on the road, such as drag and lift forces. The flow separation at the vehicle's rear end is one of the primary causes of aerodynamic drag for automobile vehicles. It is feasible to improve fuel efficiency by lowering the drag force. The study focuses on the influence of a vortex generator (VG) on the aerodynamics of a sport utility vehicle (SUV) car. The study aims to simulate fluid flow analysis for an SUV car that uses VG and without VG, as well as to assess the impact of a different configuration of VG and a varying number and fillet radius of VG. The number of VG are 3, 5, and 9. The different fillet radius of VG are 5, 10, and 15 mm. Using the Reynold-Averaged Navier Stokes Equation (RANS) in the numerical simulation, the Reynolds number at the computational domain is 1.1391×10^7 and 1.4808×10^7, which is determined by the height of the model and the freestream velocity. The results show that aerodynamic characteristics are significantly influenced by the number of VG and various size radius fillets of VG. From the result, 9 number of VG and 5 mm fillet radius obtained the lowest value of coefficient of drag, C_d compared with the others which is $C_d = 0.3747$ for 27.78 m/s and $C_d = 0.5031$ for 33.33 m/s, respectively. Furthermore, the analysis of flow structures suggested the locations of vortex formation and wake turbulence at the rear of the vehicle. In contrast, the 9 number of VG with a 5 mm radius fillet of VG emerged as the most suitable VG for this scenario, exhibiting a C_d value closest to the base model and the lowest C_d value.

1. Introduction

The preservation of energy resources and protection of the atmosphere globally significantly depend on minimizing fuel consumption in automotive development. A key strategy to enhance vehicle aerodynamics, thereby improving fuel efficiency and driving performance, is reducing the drag coefficient (Cd). Drag-reducing devices play a crucial role in achieving this goal by optimizing

---

* Corresponding author.
E-mail address: izuan@uthm.edu.my

airflow around vehicles, thereby reducing drag-inducing vortices, turbulence, and pressure imbalances [1,2].

Conducting real-world experiments is time-consuming and entails substantial financial costs. Additionally, researchers must invest considerable time to obtain results [3]. Previous research indicates that higher drag adversely affects vehicle performance, notably increasing fuel consumption. Hence, achieving a low Cd is essential for optimizing vehicle speed and stability during motion. One significant contributor to increased drag is flow separation, predominantly occurring at the rear end of vehicles due to changes in flow velocity and vehicle geometry. This phenomenon can be mitigated using aerodynamic devices such as vortex generators. Studies also suggest that higher Reynolds numbers correlate with reduced drag forces [4,5].

A significant approach in reducing aerodynamic drag and managing flow separation in vehicles involves the strategic application of vortex generators. These devices, characterized by small, fin-like structures mounted on the vehicle's surface, play a crucial role in modifying the boundary layer airflow [6]. The boundary layer refers to the thin layer of air adjacent to the vehicle's surface where significant changes in velocity and pressure occur. These devices have been shown to effectively delay flow separation, thus enhancing aerodynamic performance [7]. Research indicates that vortex generators can be passive or active, with active systems like high-frequency compliant structures producing oscillatory vortices to mitigate flow separation more effectively than static vortex generators [8]. Vortex generators have been widely used to control boundary layer separation, especially on airfoils, where they help in reactivating the boundary layer to delay airflow separation [9].

Empirical studies have demonstrated significant enhancements in airflow dynamics through the implementation of vortex generators on vehicle surfaces [10]. These generators induce vortices that facilitate momentum transfer, thereby optimizing the airflow pattern over the car's surface [11]. Research by Islam *et al.,* [10] focused on strategically placing vortex generators just upstream of the flow separation point, typically above the vehicle's rear window, to manage airflow dynamics and prevent flow separation, which can lead to increased drag and reduced aerodynamic efficiency [12].

The strategic placement of vortex generators on vehicle surfaces has been shown to be a promising approach for optimizing airflow dynamics, reducing drag, and enhancing aerodynamic efficiency [13]. Thus, this study investigates the aerodynamic performance of Vortex Generators (VGs) on SUV car models with varying numbers of VGs and VG radius fillets, considering different Reynolds Numbers. The numbers of VGs tested were 3, 5, and 9, with radius fillets of 5 mm, 10 mm, and 15 mm, respectively. The Reynolds Numbers considered were 3.0894×10^7 and 4.0163×10^7. The numerical simulations in this work employ computational fluid dynamics (CFD) in conjunction with the Reynolds-Averaged Navier Stokes Equation (RANS).

2. Methodology
2.1 Research Framework

Figure 1 illustrates the overall process flowchart and CFD analysis of this study. The 3D model of the vehicle, as shown in Figure 2, was created using SOLIDWORKS software, based on the real model of a 2012 Honda CRV SUV [14]. This model was designed to a 1:1 scale, identical to the original size manufactured by the factory. Table 1 presents three vortex generators (VGs) that are similar in shape but differ in the radius of the fillet, with r = 5 mm (case 1), r = 10 mm (case 2), and r = 15 mm (case 3). Figure 3 depicts the SUV car model with nine VGs mounted on the roof at the rear end, spaced equally. Figure 4 shows configurations with 3, 5, and 9 VGs, also spaced equally. Each VG

configuration will be tested with the same pre-processing settings and will be placed on the roof of the SUV. The VG designs were sourced from internet references [15-17].
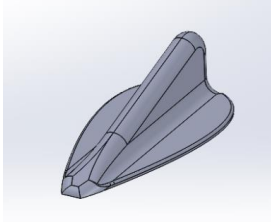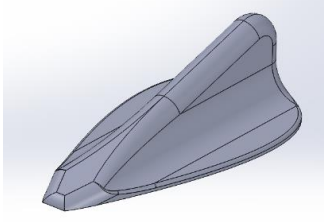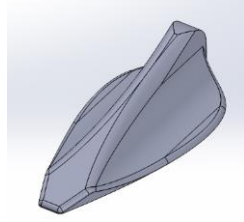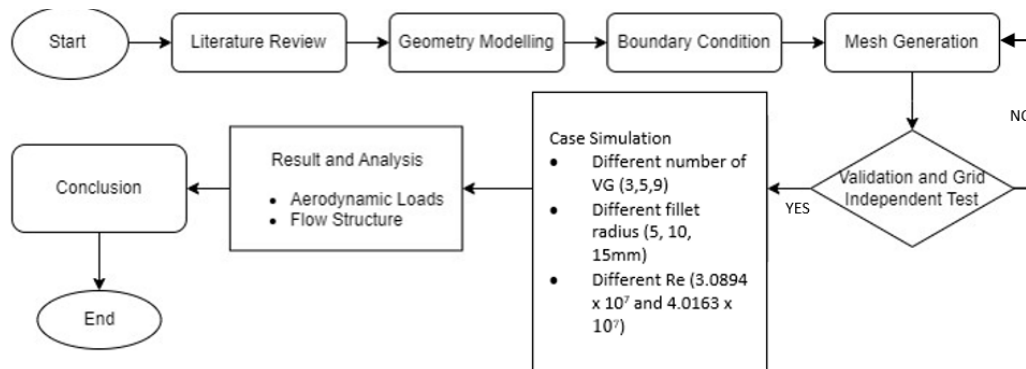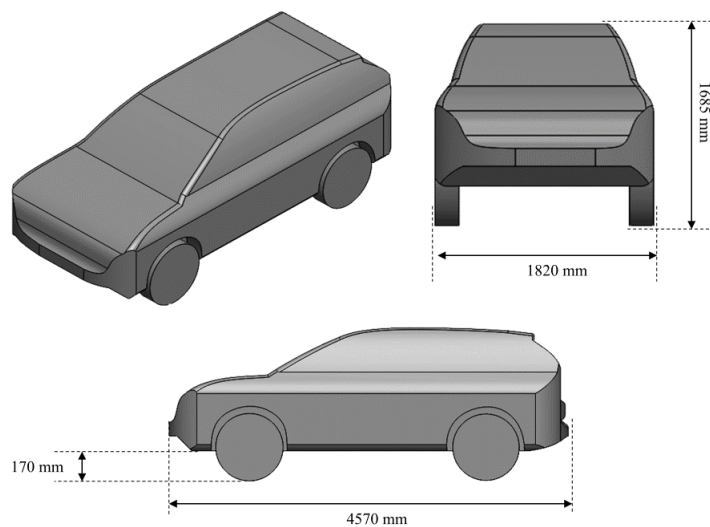

Fig. 1. Flowchart of CFD analysis

Fig. 2. The dimension of the SUV car model

Table 1
The 3 vortex generators are similar in shape but different in the radius of the fillet

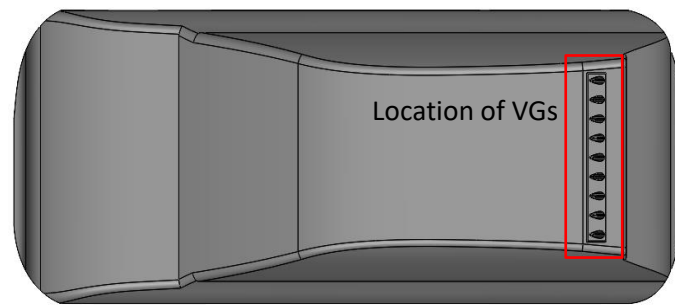|	VG-1	VG-2	VG-3
Dimensions (mm)			
Length	100	100	100
Width	50	50	50
Height	30	30	30
Thickness	10	10	10
Fillet Radius	5	10	15

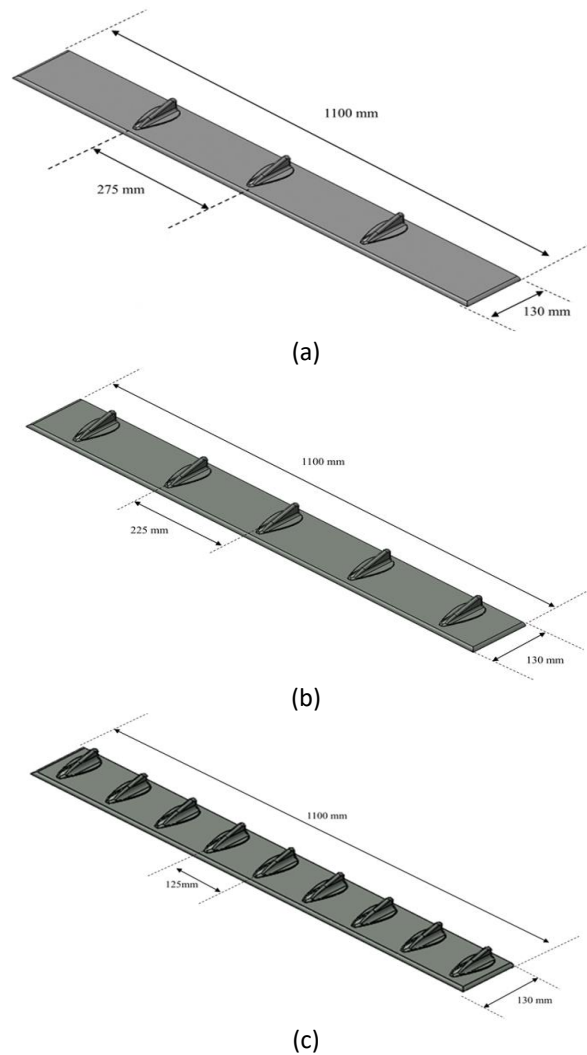**Fig. 3.** Top View of Car model with Vortex generator

(a)

(b)

(c)

Fig. 4. The dimensions of the Vortex Generator (a)
3 number of VG (b) 5 number of VG (c) 9 number
of VG

2.2 Enclosure and Boundary Conditions Used in a Simulation

In ANSYS, the enclosure size refers to the dimensions of the computational domain or the area of interest where the modeling or analysis is conducted. It is crucial to carefully select the enclosure size to ensure it sufficiently covers the area of interest for accurate results [15]. Before starting the meshing process, it is essential to confirm that the computational domain is appropriately sized. The dimensions used in this study are similar to those in previous research [14]. Figure 5 and Figure 6

illustrate the enclosure size for a vehicle used in ANSYS simulation. Table 2 provides the specific dimensions of the enclosure.
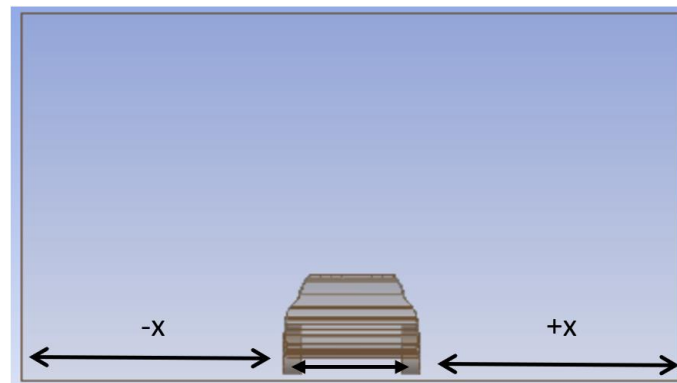

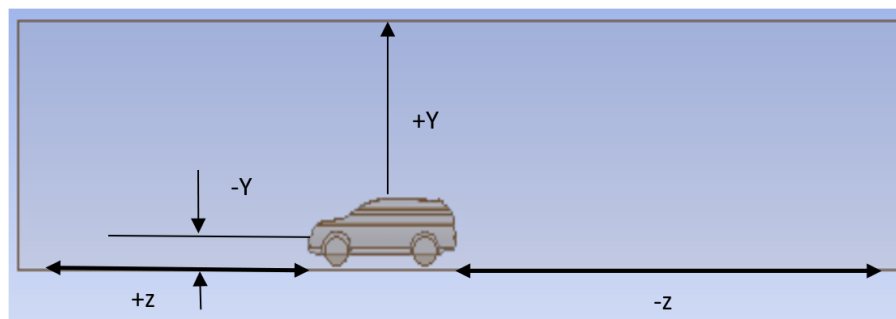**Fig. 5.** Top View of Car model with Vortex generator

Fig. 6. Side view of the enclosure for the vehicle

Table 2
Details the size of the enclosure

Plane	Dimension (m)
+X	4.57
+Y	4.57
+Z	9.00
-X	4.57
-Y	0.10
-Z	13.71

The model's boundary condition, such as velocity inlet, pressure outlet, vehicle surface, and symmetry sides, is established once the enclosure has been created as shown in Figure 7. The Reynolds number employed in this investigation is Re = 3.0894×10^7 and 4.0163×10^7, other details of boundary conditions are provided in Table 3.
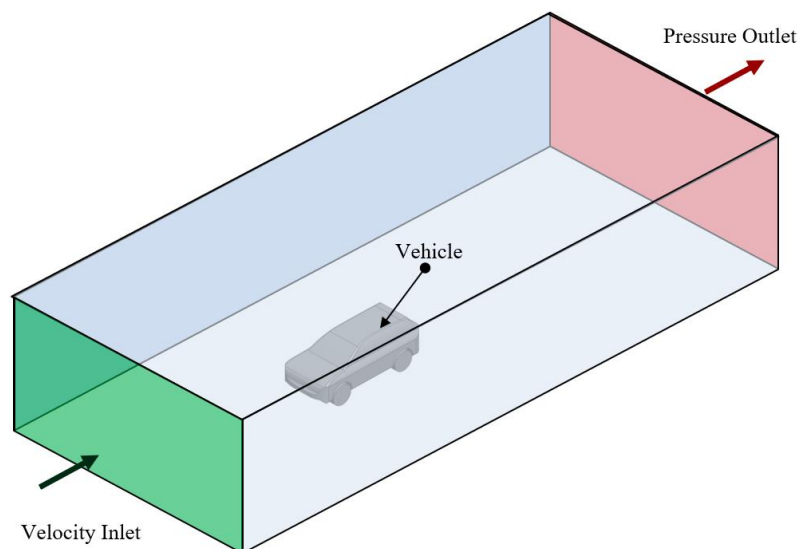
Fig. 7. The boundary conditions used in the numerical investigation

Table 3
The details for boundary conditions and the values

Detail	Boundary Condition	Value	Value
Inlet	Velocity inlet	27.78 m/s	33.33 m/s
		(3.0894×10^7)	(4.0163×10^7)
Outlet	Pressure outlet	0 Pa (gauge)	0 Pa (gauge)
Symmetry	Wall boundary	Stationary	Stationary
Vehicle Body	Wall boundary	No slip	No slip

2.3 Grid Independence Study

The CFD results were validated by comparing the drag coefficient (C_d) produced from the simulation with outcomes from three distinct mesh types. Mesh parameters were adjusted to create coarse, medium, and fine mesh types, as detailed in Table 4. Based on the obtained results, it is evident that grid dependency is achieved, as the percentage error between the medium mesh (Mesh 2) and the fine mesh (Mesh 3) is significantly small compared to coarse and medium mesh. Based on these considerations, Mesh 2 shows a balance between computational efficiency and accuracy. It offers results that closely match those obtained with the finer Mesh 3, while being computationally more feasible than Mesh 3 due to its lower node count and reduced computational demand. Therefore, Mesh 2 is chosen as the appropriate mesh configuration for the study, ensuring that the results are both accurate and efficient for further analysis and validation.

Table 4
Parameters used for validation

Mesh type	Coarse	Medium	Fine
	Mesh 1	Mesh 2	Mesh 3
Element size (mm)	1200	600	300
Body sizing (mm)	500	400	300
Face sizing (mm)	1600	800	400
Number of nodes	941217	1915591	2971795
Drag coefficient (C_d)	0.4037	0.3747	0.3735
Percentage error (%)	7.74	0.32	

3. Results and Discussion

3.1 Qualitative Result

Table 5 illustrates the changes in the drag force coefficient (C_d) with varying fillet radius of vortex generators (VG) and different numbers of VG, comparing results at velocities of inlet of 27.78 m/s and 33.33 m/s. For a velocity of inlet of 27.78 m/s without a vortex generator, the C_d value is 0.3762. In Case 1, where the VG fillet radius is 5 mm, the C_d value increases by 0.82% and 0.72% for 3 and 5 VGs, respectively, while for 9 VGs, it decreases by 0.4%. In Case 2, with a VG fillet radius of 10 mm, the C_d value increases by 5.5%, 2.1%, and 1.38% for 3, 5, and 9 VGs, respectively. In Case 3, where the VG fillet radius is 15 mm, the C_d value increases by 2.37% and 1.86% for 3 and 5 VGs, respectively, but decreases by 0.98% for 9 VGs.

For a velocity inlet of 33.33 m/s without a vortex generator, the C_d value is 0.5386. In Case 1, with a VG fillet radius of 5 mm, the C_d value increases by 5.27% for 3 VGs but decreases by 0.91% and 6.59% for 5 and 9 VGs, respectively. In Case 2, with a VG fillet radius of 10 mm, the C_d value increases by 8.28%, 6.15%, and 5.07% for 3, 5, and 9 VGs, respectively. In Case 3, with a VG fillet radius of 15 mm, the C_d value increases by 2.38% and 2.30% for 3 and 5 VGs, respectively, but decreases by 0.45% for 9 VGs.

The data from Figure 8, Figure 9, and Table 5 indicate that certain configurations and numbers of VGs can be used on SUV cars to achieve the lowest C_d value.
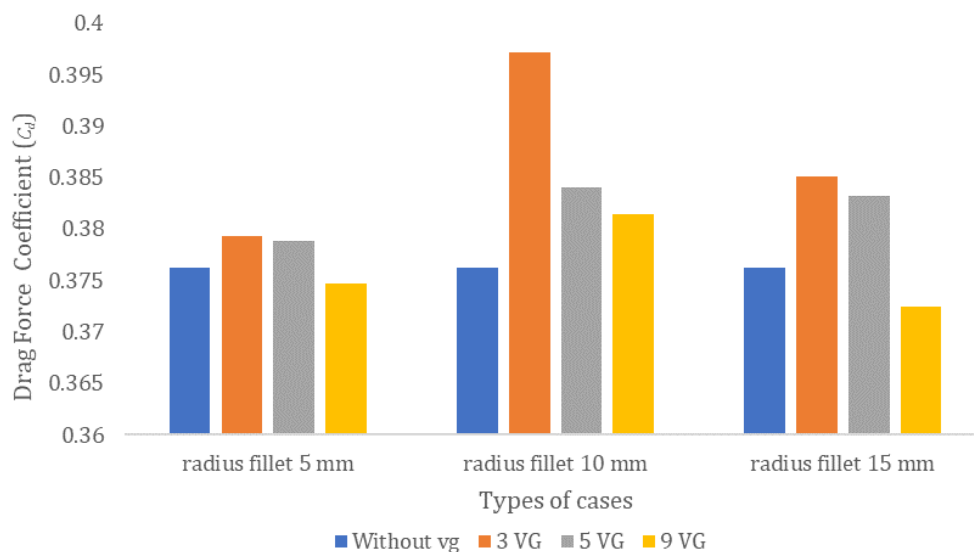

Fig. 8. Graph of drag coefficient (C_d) for with and without VG at inlet velocity of 27.78 m/s
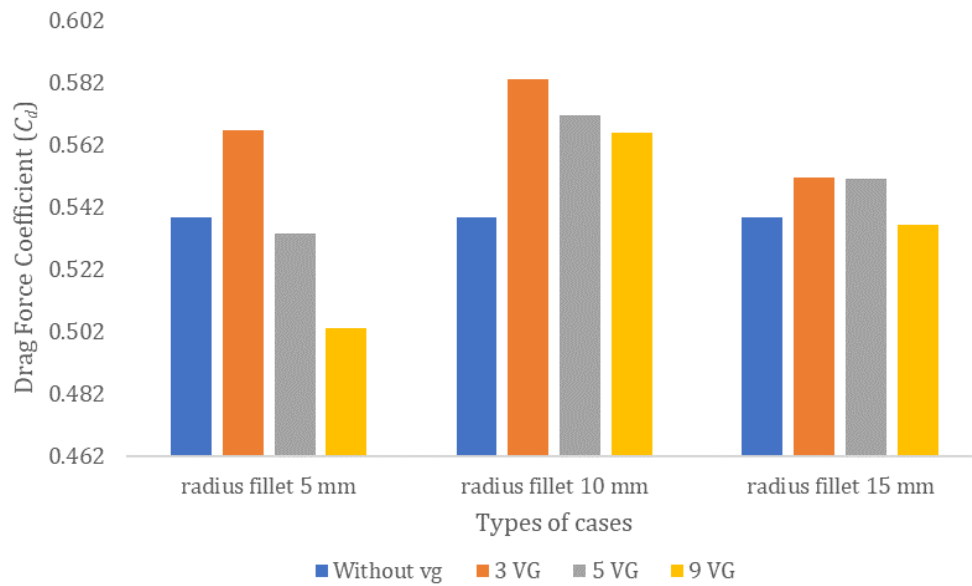
Fig. 9. Graph of drag coefficient (C_d) for with and without VG at inlet velocity 33.33 m/s

Table 5
The Different Drag Coefficient (C_d) between inlet velocity of 27.78 m/s and 33.33 m/s

| Types	No. of Vortex Generator	Drag coefficient	
		Speed	
		27.78 m/s	33.33 m/s
Base model	Without VG	0.3762	0.5386
Case 1 (r = 5 mm)	3	0.3793	0.5670
	5	0.3789	0.5337
	9	0.3747	0.5031
Case 1 (r = 10 mm)	3	0.3972	0.5832
	5	0.3841	0.5717
	9	0.3814	0.5659
Case 1 (r = 15 mm)	3	0.3851	0.5514
	5	0.3832	0.5510
	9	0.3725	0.5362

3.2 Quantitative Result

3.2.1 Flow structure analysis when velocity is 27.78 m/s

Figure 10 shows the pressure contour generated in the symmetry plane by the SUV car model. The results indicate that the length of the maximum pressure region for 3 and 5 vortex generators (VGs) is almost the same, with the 3 VG configuration having a slightly longer high-pressure region than the 5 VG configuration. For the 9 VG configuration, the length of the high-pressure region behind the VGs increases compared to the 3 and 5 VG configurations. Additionally, the streamline analysis shows that with 9 VGs, the airflow is more attached to the rear surface of the SUV than with 3 or 5 VGs. This is due to the lower pressure behind the SUV, which disrupts the smoothness of the airflow over the surface. This trend corresponds with the observed decrease in the drag coefficient (C_d) from 3 to 9 VGs mounted on the SUV. This phenomenon was attributed to the lower pressure behind the SUV, which disrupted the smoothness of the airflow over the surface, leading to a decrease in the drag coefficient (Cd) [18].
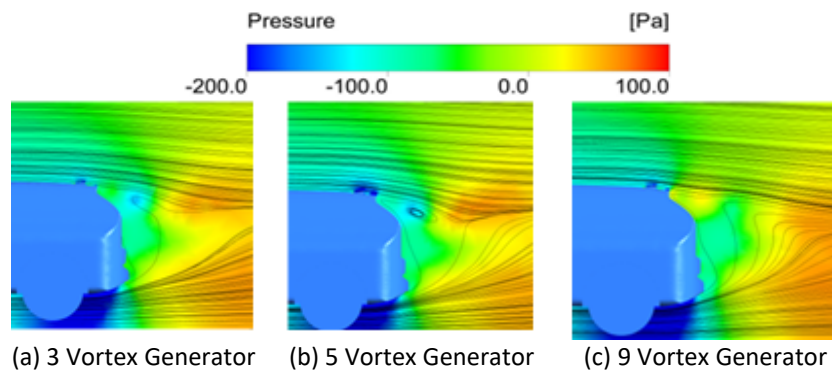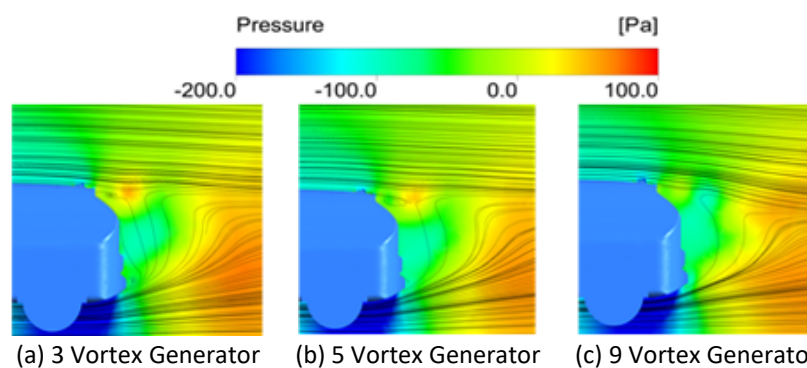
(a) 3 Vortex Generator   (b) 5 Vortex Generator   (c) 9 Vortex Generator
Fig. 10. Pressure contour superimposed with streamline for radius fillet of VG: 5 mm with different number of VG

Figure 11 presents the pressure contour superimposed with streamlines for a VG fillet radius of 10 mm and different numbers of VGs. The pressure contours appear almost identical for the 3, 5, and 9 VG configurations, reflecting the minor changes in the drag coefficient among these cases. The streamline analysis shows that the 3 and 5 VG configurations create larger vortex turbulence wake regions behind the SUV compared to the 9 VG configuration [19].
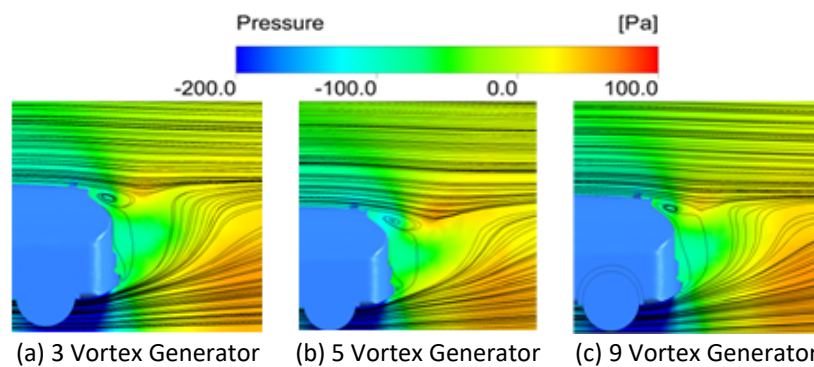
(a) 3 Vortex Generator   (b) 5 Vortex Generator   (c) 9 Vortex Generator
Fig. 11. Pressure contour superimposed with streamline for radius fillet of VG: 10 mm with different number of VG
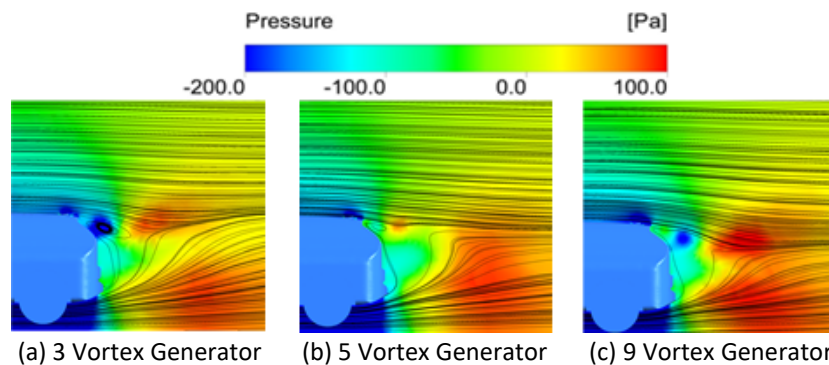
Figure 12 depicts the pressure contour superimposed with streamlines for a VG fillet radius of 15 mm with varying numbers of VGs. The results show an increase in the length of the high-pressure region behind the VGs as the number of VGs increases, similar to the trend observed in Figure 10. The streamlines indicate more turbulence in the 3 and 5 VG configurations compared to the 9 VG configuration. This smoother airflow behind the SUV with 9 VGs helps reduce the drag coefficient.

(a) 3 Vortex Generator   (b) 5 Vortex Generator   (c) 9 Vortex Generator
Fig. 12. Pressure contour superimposed with streamline for radius fillet of VG: 15 mm with different number of VG
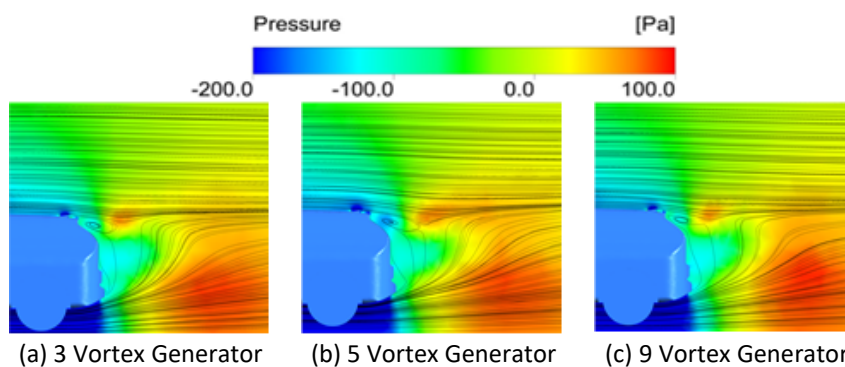
3.2.2 Flow structure analysis when velocity is 33.33 m/s

Figure 13 shows the pressure contour superimposed with streamlines for a VG fillet radius of 5 mm with different numbers of VGs. The results indicate that the high-pressure region is closest to the SUV for the 5 VG configuration, followed by the 3 VG configuration, and furthest for the 9 VG configuration. The 9 VG configuration also exhibits smoother and more attached flow streamlines at the rear of the car compared to the other configurations. This smoother airflow corresponds with the lowest drag coefficient (C_d) observed for the 9 VG configuration, as shown in Table 5.

(a) 3 Vortex Generator   (b) 5 Vortex Generator   (c) 9 Vortex Generator

Fig. 13. Pressure contour superimposed with streamline for radius fillet of VG: 5 mm with different number of VG

Figure 14 presents the pressure contour superimposed with streamlines for a VG fillet radius of 10 mm with varying numbers of VGs. The pressure contours appear almost identical for the 3, 5, and 9 VG configurations, reflecting the minor changes in the drag coefficient among these cases. The streamline analysis shows that the 9 VG configuration results in smoother flow and smaller wake vortices, leading to better attachment of the flow on the rear car surface. This results in a reduced drag coefficient, as indicated in Table 5.

(a) 3 Vortex Generator   (b) 5 Vortex Generator   (c) 9 Vortex Generator

Fig. 14. Pressure contour superimposed with streamline for radius fillet of VG: 10 mm with different number of VG

Figure 15 depicts the pressure contour superimposed with streamlines for a VG fillet radius of 14 mm with different numbers of VGs. The distance between the highest-pressure region and the back of the car increases with the number of VGs. Additionally, the flow streamlines indicate more turbulence for the 3 and 5 VG configurations compared to the 9 VG configuration. The smoother airflow behind the SUV in the 9 VG configuration helps reduce the drag coefficient.
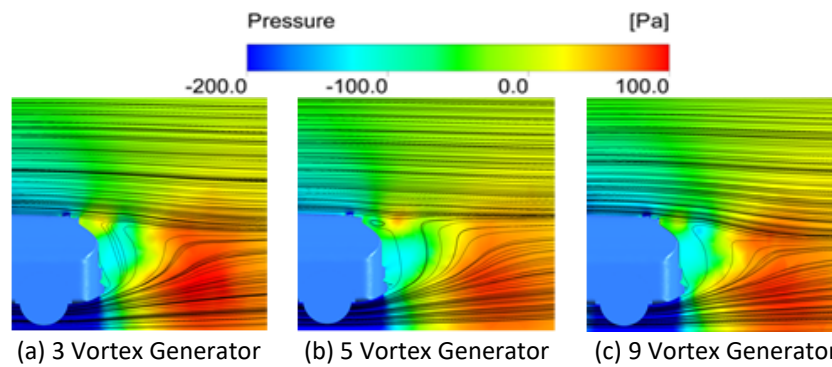
(a) 3 Vortex Generator (b) 5 Vortex Generator (c) 9 Vortex Generator

Fig. 15. Pressure contour superimposed with streamline for radius fillet of VG: 15 mm with different number of VG

3.2.3 Flow structure from top view at 27.78 m/s

Figure 16 shows the pressure contour superimposed with streamlines from a top view for a VG fillet radius of 5 mm with different numbers of VGs. The structure length between the rear of the SUV and the high-pressure region increases in ascending order from 3 to 5 to 9 VGs. For the 9 VG configuration, the pressure on the rear of the SUV is lower compared to the other two cases. This is because the stronger and more numerous vortices in this configuration create a high-pressure region further away from the rear of the SUV, pushing the air away more effectively.
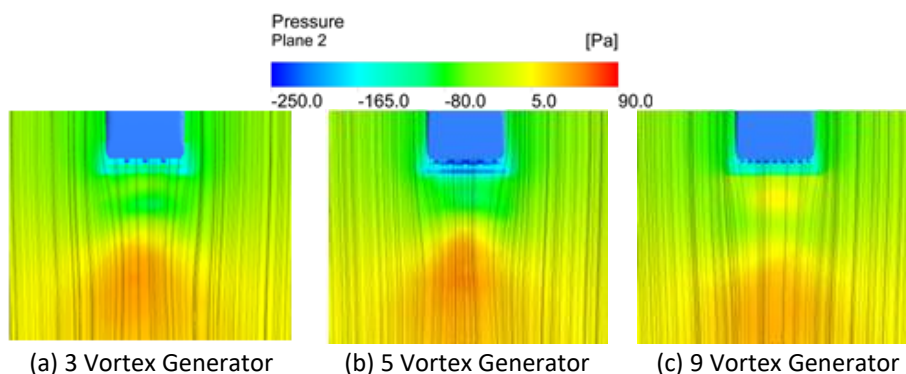

(a) 3 Vortex Generator (b) 5 Vortex Generator (c) 9 Vortex Generator

Fig. 16. Pressure contour superimposed with streamline for radius fillet of VG: 5 mm with different numbers of VG at the top view

Figure 17 illustrates the pressure contour superimposed with streamlines from a top view for a VG fillet radius of 10 mm with different numbers of VGs. In this case, the structure length between the rear VGs and the high-pressure region is almost the same for 3, 5, and 9 VGs, which aligns with the minor changes in the drag coefficient (C_d). However, the 9 VG configuration still shows lower pressure on the rear of the SUV compared to the other configurations. This is due to the stronger and more vortices in the 9 VG case, which push the high-pressure region further from the SUV. The 10 mm fillet radius creates the highest pressure in the 9 VG configuration compared to the other two configurations.
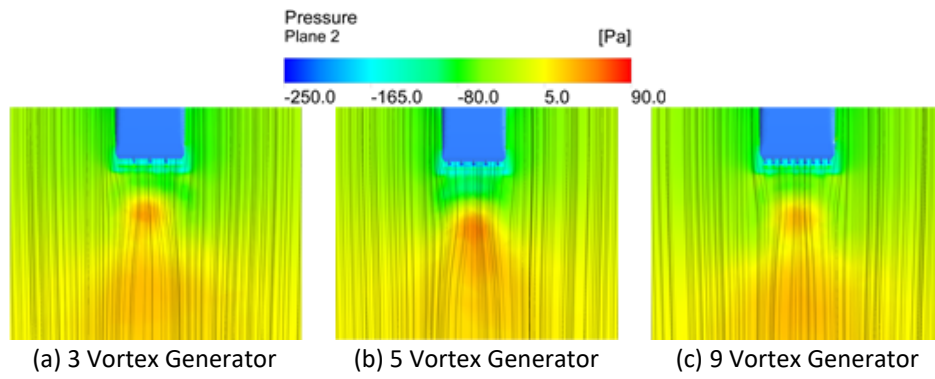
(a) 3 Vortex Generator   (b) 5 Vortex Generator   (c) 9 Vortex Generator

Fig. 17. Pressure contour superimposed with streamline for radius fillet of VG:
10 mm with different numbers of VG at the top view

Figure 18 shows the pressure contour superimposed with streamlines from a top view for a VG fillet radius of 15 mm with different numbers of VGs. The structure length between the rear of the SUV and the high-pressure region increases in ascending order from 3 to 5 to 9 VGs. In the 9 VG configuration, the pressure on the rear of the SUV is lower than in the other two configurations. This is because the stronger and more vortices in the 9 VG configuration create a high-pressure region further away from the rear of the SUV, thus reducing drag more effectively. This trend is consistent with the pressure contours showing higher pressure regions further from the SUV in the 9 VG case compared to the 3 and 5 VG cases.
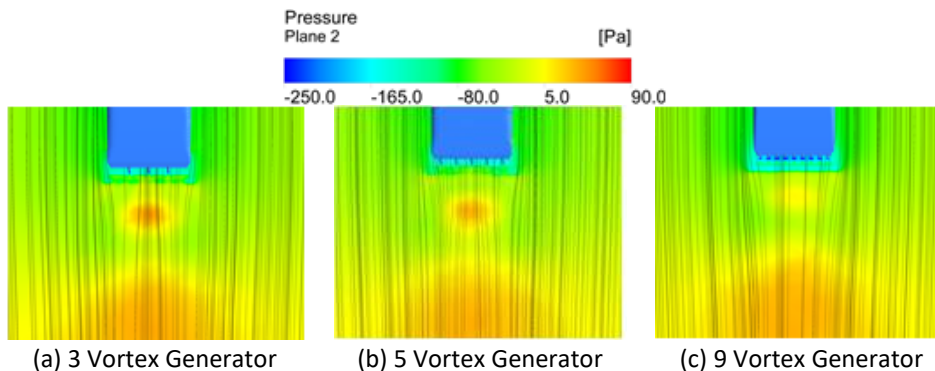

(a) 3 Vortex Generator   (b) 5 Vortex Generator   (c) 9 Vortex Generator

Fig. 18. Pressure contour superimposed with streamline for radius fillet of VG:
15 mm with different numbers of VG at the top view

3.2.4 Flow structure from top view at 33.33 m/s

Figure 19 shows the pressure contour superimposed with streamlines from a top view for a VG fillet radius of 5 mm with different numbers of VGs. The structure length between the rear of the SUV and the high-pressure region increases in ascending order from 3 to 5 to 9 VGs. For the 9 VG configuration, the pressure on the rear of the SUV is lower than in the other two cases. This is because the stronger and more numerous vortices in this configuration create a high-pressure region further away from the rear of the SUV, effectively pushing the air away from the rear of the car.
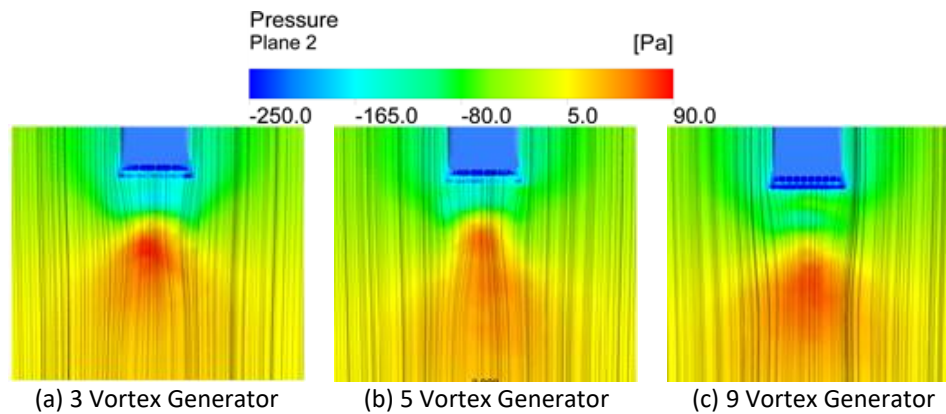
(a) 3 Vortex Generator   (b) 5 Vortex Generator   (c) 9 Vortex Generator

Fig. 19. Pressure contour superimposed with streamline for radius fillet of VG: 5 mm with different numbers of VG at the top view

Figure 20 illustrates the pressure contour superimposed with streamlines from a top view for a VG fillet radius of 10 mm with different numbers of VGs. The structure length between the rear of the car and the high-pressure region is nearly the same for the 3, 5, and 9 VG configurations, reflecting the small changes in the drag coefficient (C_d). However, for the 9 VG configuration, the pressure on the rear of the SUV is lower than in the other two cases. Additionally, the 5 VG configuration creates the highest pressure compared to the other two cases.
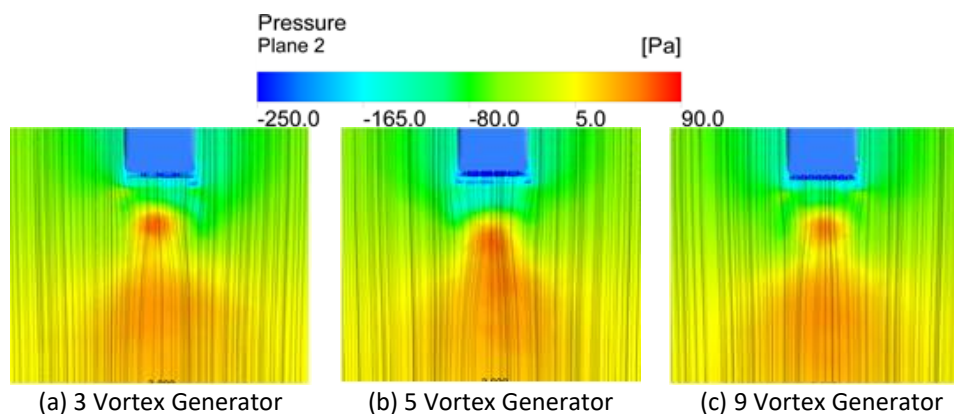

(a) 3 Vortex Generator   (b) 5 Vortex Generator   (c) 9 Vortex Generator

Fig. 20. Pressure contour superimposed with streamline for radius fillet of VG: 10 mm with different numbers of VG at the top view

Figure 21 shows the pressure contour superimposed with streamlines from a top view for a VG fillet radius of 15 mm with different numbers of VGs. The structure length between the rear of the SUV and the high-pressure region increases in ascending order from 3 to 5 to 9 VGs. In the 9 VG configuration, the pressure on the rear of the SUV is lower than in the other two cases, which show a highest-pressure contour followed by the 5 and 3 VG configurations. Increasingly the number and strength of vortices, as observed in a 9 VGs configuration compared to 3 VGs, creates a high-pressure region further away from the vehicle. This high-pressure region aids in reducing the drag force acting on the vehicle [6,20,21].
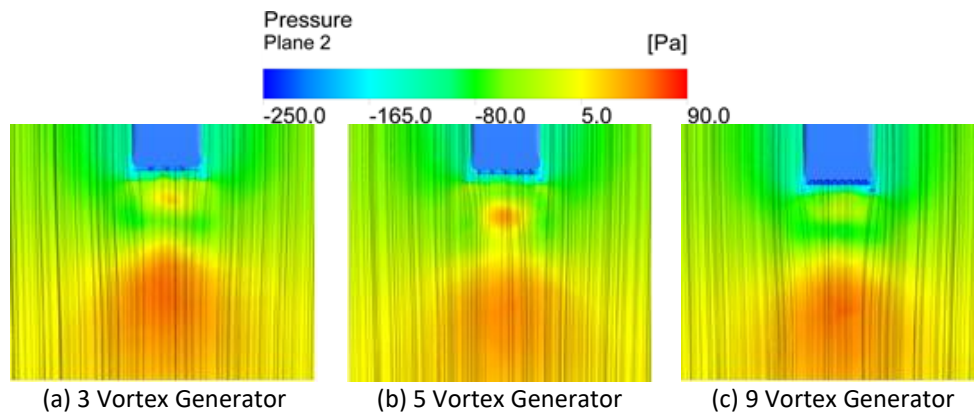
(a) 3 Vortex Generator   (b) 5 Vortex Generator   (c) 9 Vortex Generator

Fig. 21. Pressure contour superimposed with streamline for radius fillet of VG: 15 mm with different numbers of VG at the top view

3.2.5 Flow structure on the Vortex Generator

Figure 22 displays the pressure contour bar for a velocity of 27.78 m/s, where the blue colour represents the lowest pressure at -250.0 Pa, and the red colour represents the highest pressure at -60.0 Pa. In this figure, Case A, with a fillet radius of VG of 5 mm, exhibits the lowest pressure region compared to Case B and Case C. Within Case A, it can be observed that the configuration with 3 VGs has the smallest low-pressure region after the air passes through it, followed by the configuration with 5 VGs, which has a slightly larger low-pressure region compared to the 3 VG configuration. Lastly, the configuration with 9 VGs shows the largest size of the low-pressure region after the air passes through it. This phenomenon occurs because the smaller fillet radius and the larger number of VGs create stronger and more vortices. The enhanced strength of the vortices facilitates the disruption of the smooth airflow over the car, thereby contributing to improved aerodynamics by reducing drag and enhancing overall performance [22].

Figure 23 displays pressure contours at 33.33 m/s, where blue represents the lowest pressure of -400 Pa and red indicates the highest pressure of -150 Pa. It shows that with 3 vortex generators (VGs), pressure is highest at the VG's rear due to less uniform pressure distribution compared to 5 and 9 VG configurations. With 9 VGs, pressure distribution is more uniform around the VGs, indicating better airflow attachment to the car surface and improved aerodynamics. In Case A (5 mm fillet radius with 9 VGs), the highest-pressure region is directly above the VGs due to strong vortices generated by the small fillet radius and multiple VGs. These vortices create a low-pressure area above the VGs, disrupting airflow and potentially enhancing car aerodynamics.
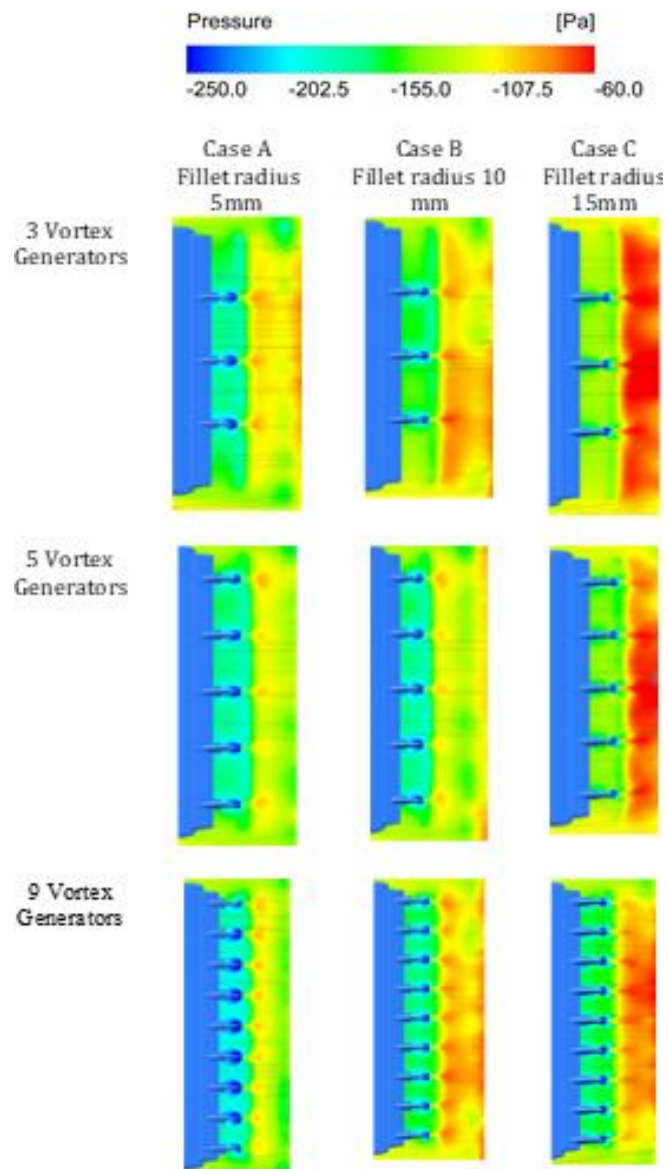
Fig. 22. Up close view of pressure contour superimposes with streamline for 3 different numbers of VG with different fillet radius at Reynold number 27.28 m/s
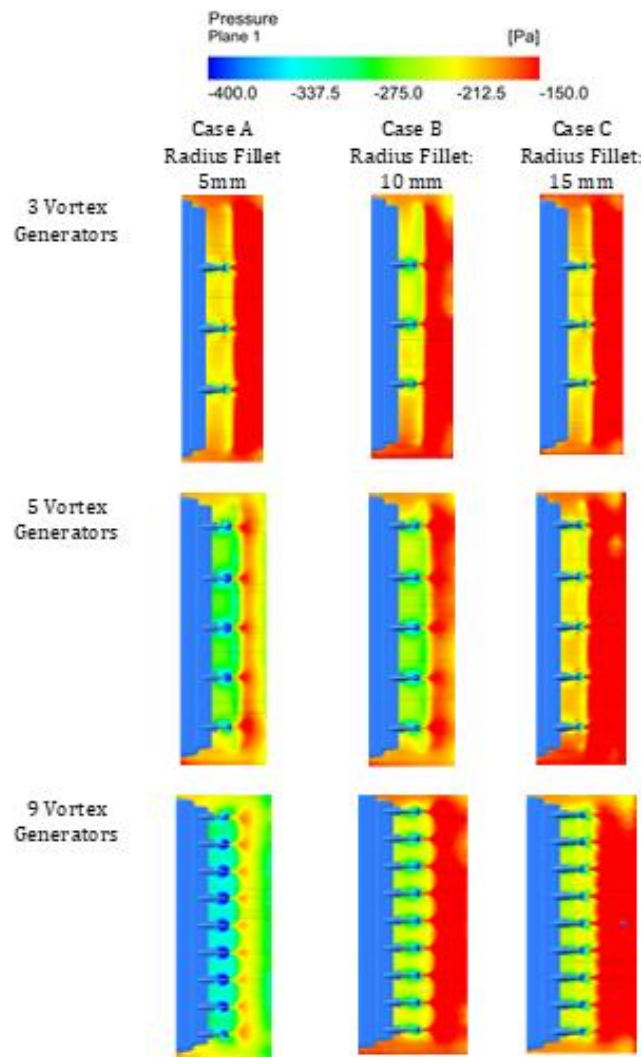
Fig. 23. Up close view of pressure contour superimposes with streamline for 3 different numbers of VG with different fillet radius at Reynold number 33.33 m/s

4. Conclusion

In conclusion, utilizing Computational Fluid Dynamics (CFD) analysis to study vortex generators (VGs) in cars proves promising for enhancing vehicle efficiency. The findings demonstrate that VGs effectively reduce the drag coefficient (C_d) compared to the base model.

The simulations show that using 9 VGs results in the most favorable aerodynamic outcomes, with reductions in C_d percentages compared to the base model. Specifically, at an inlet speed of 27.78 m/s, configurations with 9 VGs and fillet radii of 5 mm and 15 mm exhibit the lowest C_d values, showing reductions of 0.4% and 0.98%, respectively, compared to the base model. Similarly, at a speed of 33.33 m/s, configurations with 9 VGs and fillet radii of 5 mm and 15 mm demonstrate reductions of 0.91% and 0.45% in C_d, respectively, compared to the base model.

Furthermore, regarding flow structure, VGs effectively delay flow separation. Configurations with 9 VGs on an SUV car show an increased distance of the higher-pressure region from the rear, resulting in lower rear pressure compared to configurations with 3 and 5 VGs. This pressure distribution directly influences aerodynamic load, highlighting the importance of reducing turbulence to decrease drag and emphasizing the interconnectedness of aerodynamic drag, turbulence, and airflow patterns.

Overall, the configuration of 9 VGs with a fillet radius of 5 mm emerges as the optimal choice for achieving efficient aerodynamic flows, consistently yielding the lowest C_d values compared to the base model.

Acknowledgement

References

[1] Gopal, P., T. Senthilkumar, and C. Rameshkumar. "Aerodynamic drag reduction in a passenger vehicle using vortex generator with varying yaw angles." *ARPN Journal of Engineering and Applied Sciences* 7, no. 9 (2012): 1180-1186.

[2] Sen, Wriddha, Kazi Afzalur Rahman, and Ibrahim Khalil Tanim. "Experimental and CFD analysis on car with several types of vortex generators." In *Proceedings of the International Conference on Mechanical Engineering and Renewable Energy*, pp. 11-13. 2019.

[3] Simscale. "What is CFD | Computational Fluid Dynamics?." *Simscale*.

[4] Fernández Gámiz, Unai. "Fluid dynamic characterization of vortex generators and two-dimensional turbulent wakes." *PhD diss., Universitat Politècnica de Catalunya (UPC)*, 2013.

[5] Shivam, Sidharth Singh, Abhishek Guleria, and Yagna S. Mukkamala. "Aerodynamic Drag Reduction of a Notchback Car Geometry by Delaying Flow Separation using Vortex Generators." *International Journal of Engineering Research & Technology (IJERT)* 4, no. 8 (2015): 521-524. https://doi.org/10.17577/IJERTV4IS080447

[6] Hares, H., G. Mebarki, M. Brioua, and M. Naoun. "Aerodynamic performances improvement of NACA 4415 profile by passive flow control using vortex generators." *Journal of the Serbian Society for Computational Mechanics* 13, no. 1 (2019): 17-38. https://doi.org/10.24874/jsscm.2019.13.01.02

[7] Kerho, M., S. Hutcherson, R. F. Blackwelder, and R. H. Liebeck. "Vortex generators used to control laminar separation bubbles." *Journal of Aircraft* 30, no. 3 (1993): 315-319. https://doi.org/10.2514/3.46336

[8] Kota, Sridhar, Michael Lee, Donald Geister, Russell Osborn, and Carl Tilmann. "Active flow control using high frequency compliant structures." In *AIAA Guidance, Navigation, and Control Conference and Exhibit*, p. 4144. 2001. https://doi.org/10.2514/6.2001-4144

[9] Li, Songlin, Junwen Shao, and Yuze Sun. "Study on vortex generator on automobile and airplane." *Theoretical and Natural Science* 26, no. 1 (2023): 139-144. http://doi.org/10.54254/2753-8818/26/20241049

[10] Islam, Md Rasedul, Md Amzad Hossain, Mohammad Mashud, and Md Tanvir Ibny Gias. "Drag reduction of a car by using vortex generator." *International Journal of Scientific & Engineering Research* 4, no. 7 (2013): 1298-1302.

[11] Elsayed, Omer, Ashraf A. Omar, Ali Jeddi, Saad El Hessni, and Fatima Zahra Hachimy. "Drag reduction by application of different shape designs in a sport utility vehicle." *International Journal of Automotive and Mechanical Engineering* 18, no. 3 (2021): 8870-8881. https://doi.org/10.15282/ijame.18.3.2021.03.0680

[12] Joseph, Katz, Darwin Garcia, and Robin Sluder. *Aerodynamics of race car liftoff*. No. 2004-01-3506. SAE Technical Paper, 2004. https://doi.org/10.4271/2004-01-3506

[13] Krishna, Bese Gopi, and Samsani Durga Prasad. "Design and Analysis of Vortex Generators." *International Journal for Modern Trends in Science and Technology* 4, no. 2 (2018): 25-31.

[14] Ismail, Muhammad Pirdaus, Izuan Amin Ishak, Nor Afzanizam Samiran, Ahmad Faiz Mohammad, Zuliazura Mohd Salleh, and Nofrizalidris Darlis. "CFD analysis on the effect of vortex generator on sedan car using ANSYS software." *International Journal of Integrated Engineering* 14, no. 1 (2022): 73-83.

[15] Azwari, Nur Farhanatul Syasya Mohd, and Abdul Azeez Kadar Hamsa. "Evaluating actual speed against the permissible speed of vehicles during free-flow traffic conditions." *Jurnal Kejuruteraan* 33, no. 2 (2021): 183-191. https://doi.org/10.17576/jkukm-2021-33(2)-03

[16] Selvaraju, P. N., and D. Satish Kumar. "Effect of external devices on aerodynamic performance of SUV car model." *Materials Today: Proceedings* 68 (2022): 1273-1279. https://doi.org/10.1016/j.matpr.2022.06.235

[17] Hetawal, Sneh, Mandar Gophane, B. K. Ajay, and Yagnavalkya Mukkamala. "Aerodynamic study of formula SAE car." *Procedia Engineering* 97 (2014): 1198-1207. https://doi.org/10.1016/j.proeng.2014.12.398

[18] Selvaraju, P. N., and K. M. Parammasivam. "Empirical and numerical analysis of aerodynamic drag on a typical SUV car model at different locations of vortex generator." *Journal of Applied Fluid Mechanics* 12, no. 5 (2019): 1487-1496. https://doi.org/10.29252/jafm.12.05.29674

[19] Kumar, Mohan Jagadeesh, Anoop Dubey, Shashank Chheniya, and Amar Jadhav. "Effect of Vortex generators on Aerodynamics of a Car: CFD Analysis." *International Journal of Innovations in Engineering and Technology (IJIET)* 2, no. 1 (2013): 137-144.

[20] Jantzen, Ryan T., Kunihiko Taira, Kenneth O. Granlund, and Michael V. Ol. "Vortex dynamics around pitching plates." *Physics of Fluids* 26, no. 5 (2014). https://doi.org/10.1063/1.4879035

[21] Li, Xinkai, Ke Yang, and Xiaodong Wang. "Experimental and numerical analysis of the effect of vortex generator height on vortex characteristics and airfoil aerodynamic performance." *Energies* 12, no. 5 (2019): 959. https://doi.org/10.3390/en12050959

[22] Shankar, G., G. Devaradjane, and S. Sunil. "Investigation on aerodynamic behaviour of a SUV car model with vortex generators at different yaw conditions." *Journal of Applied Fluid Mechanics* 12, no. 1 (2019): 103-117. https://doi.org/10.29252/jafm.75.253.28851